Received: 12 May 2023 | Revised: 7 September 2023 | Accepted: 2 October 2023

DOI: 10.1002/psp4.13064

ARTICLE

Population pharmacokinetic and exposure-response analyses of pemigatinib in patients with advanced solid tumors including cholangiocarcinoma

Xiaohua Gong[1] | **Ayman Akil**[2] | **Andre Ndi**[2] | **Tao Ji**[3] | **Xiang Liu**[1] | **Mark Lovern**[2] | **Xuejun Chen**[1]

[1]Incyte Research Institute, Wilmington, Delaware, USA

[2]Certara Strategic Consulting, Princeton, New Jersey, USA

[3]Allorion Therapeutics, Natick, Massachusetts, USA

Correspondence
Xiaohua Gong, Incyte Research Institute, 1815 Augustine Cut-Off, Wilmington, DE 19803, USA.
Email: xgong@incyte.com

Abstract

Pemigatinib is a selective, potent, oral inhibitor of fibroblast growth factor receptor (FGFR)1–3 with efficacy in patients with previously treated, advanced/metastatic cholangiocarcinoma (CCA) with *FGFR2* alterations. A previously developed population pharmacokinetic (PK) model of pemigatinib was refined using an updated dataset with 467 participants from seven clinical studies, including patients with CCA. Updated PK model parameters were used to evaluate the association between pemigatinib exposure and efficacy and safety. Pemigatinib PK was adequately described by a two-compartment model with linear elimination and sequential zero- and first-order absorption. The final model successfully minimized, had a successful covariance step, and showed unbiased goodness-of-fit. Estimated first-order absorption rate constant and apparent clearance were 3.7/h and 10.7 L/h, respectively. Sex, baseline body weight, and concomitant use of phosphate binders, proton pump inhibitors, or histamine-2 antagonists significantly impacted PK parameters; however, the impact of covariates on PK exposure was not clinically significant. Steady-state pemigatinib exposure and mean change from baseline in serum phosphate concentration were associated with objective response rate in a bell-shaped relationship and were significantly associated with increased hyperphosphatemia. Pemigatinib exposure was associated with treatment-emergent adverse events, such as decreased appetite, nausea, and stomatitis, although the relationships were shallow. Overall, analyses indicate that 13.5 mg pemigatinib once daily in 21-day cycles (2 weeks on, 1 week off) offers a favorable benefit–risk profile in patients with advanced/metastatic or surgically unresectable CCA and is the optimal dose for clinical development.

Study Highlights

WHAT IS THE CURRENT KNOWLEDGE ON THIS TOPIC?

Pemigatinib, a fibroblast growth factor receptor (FGFR)1–3 inhibitor, is approved to treat adults with previously treated, unresectable or locally advanced/metastatic cholangiocarcinoma with *FGFR2* fusions/re-arrangements and relapsed/refractory myeloid/lymphoid neoplasms (MLNs) with *FGFR1* re-arrangement.

WHAT QUESTION DID THIS STUDY ADDRESS?

A population pharmacokinetic (PK) model for pemigatinib was previously developed; however, new data, including PK data from patients with MLN with *FGFR1* re-arrangement, are now available. We also developed efficacy and safety exposure-response models for patients with cholangiocarcinoma with *FGFR2* re-arrangements.

WHAT DOES THIS STUDY ADD TO OUR KNOWLEDGE?

Our updated population PK model of pemigatinib in patients with both solid and hematologic malignancies was a two-compartment model with sequential zero- and first-order absorption and linear elimination. Higher pemigatinib exposure as well as baseline serum phosphate concentrations are associated with both increased hyperphosphatemia and efficacy.

HOW MIGHT THIS CHANGE DRUG DISCOVERY, DEVELOPMENT, AND/OR THERAPEUTICS?

This study demonstrates how combining population PK analysis with efficacy and safety exposure-response modeling can be used to determine the optimal dose of pemigatinib for the treatment of cholangiocarcinoma.

INTRODUCTION

Fibroblast growth factor receptors (FGFR) regulate multiple cellular processes.[1] Somatic *FGFR* alterations, including amplifications, re-arrangements, and activating mutations, may lead to dysregulated ligand-independent FGFR signaling and tumor development.[2] Clinically actionable *FGFR* alterations have been identified in many solid tumors, including cholangiocarcinoma (CCA)[3] and in myeloid/lymphoid neoplasms (MLNa).[4] FGFR inhibition is therefore a rational targeted therapy for many cancers.

Pemigatinib is an oral, potent, selective FGFR1–3 inhibitor with antitumor activity in multiple solid tumors[5,6] and MLN with *FGFR1* re-arrangement (MLN^{FGFR1}).[7,8] Hyperphosphatemia is a known on-target pharmacologic effect of FGFR inhibition and is among the most commonly reported adverse events associated with treatment.[9] Pemigatinib is approved in the United States for adults with previously treated, unresectable, locally advanced or metastatic CCA with an *FGFR2* fusion or other re-arrangement, and adults with relapsed or refractory MLN^{FGFR1}.[10]

A previous pharmacokinetic (PK) analysis in patients with advanced malignancies demonstrated rapid and near-complete absorption and low renal clearance of pemigatinib.[11] In vitro, cytochrome P450 (CYP) 3A metabolized pemigatinib, and in healthy participants, co-administration of a strong CYP3A4 inhibitor or inducer resulted in clinically significant changes in exposure.[12] Organ impairment studies have shown clinically significant increases in pemigatinib exposure in patients with severe hepatic or renal impairment.[13]

A population PK analysis of pemigatinib in patients with advanced solid tumors was recently reported.[14] PK was adequately described as a two-compartment disposition model with first-order absorption and linear elimination. Female sex and concomitant use of a phosphate binder were found to decrease pemigatinib clearance, but effects were not clinically meaningful. No dose adjustments were recommended for patients with mild or moderate renal or hepatic impairment. Exposure-response (E-R) analyses of efficacy and safety in patients with CCA were also previously reported.[6] However, patients with MLN^{FGFR1} were not included in the PK analysis. The purpose of this study is to update the population PK model with additional data from more recent studies, refine the absorption model for better characterization of peak concentrations, identify and characterize factors that influence pemigatinib exposure, and update efficacy and safety E-R models for patients with CCA with *FGFR2* fusions/re-arrangements.

METHODS

Clinical study data for population PK analysis

Data from seven clinical studies, which included healthy participants and patients with CCA, other solid tumors or MLN^{FGFR1}, were used for the population PK analysis (Table S1). All studies were performed in accordance with the International Council for Harmonization Good Clinical Practice, the principles embodied by the Declaration of Helsinki, and local regulatory requirements. The study protocol and all amendments were reviewed and approved by the institutional review board of each site before patient enrollment. Patients provided written informed consent.

Population PK analysis

Plasma samples were analyzed using a validated, liquid chromatography–tandem mass spectrometry method, as previously described. Nonlinear mixed-effects modeling (NONMEM) version 7.4.3 (ICON) was used for population PK modeling with PsN version 7.4.3 (Department of Pharmacy, Uppsala University) used for model diagnostics and to facilitate covariate testing in NONMEM. Model code is provided in the Appendix S1. Graphical analysis, model diagnostics, statistical summaries, and linear or nonlinear regression analysis were performed in R version 4.1.0 (The R Foundation for Statistical Computing).[15]

The pemigatinib population PK two-compartment model with linear absorption and elimination previously developed with data from FIGHT-101 ($n=157$), FIGHT-102 ($n=25$), and FIGHT-202 ($n=136$) was refined. Interindividual random effects were kept the same as in the original model. The following covariates were tested: sex, age at baseline, use of phosphate-binding agents, use of CYP3A4 inducers or inhibitors, participant type (healthy participants; patients with CCA, other solid tumors, or MLN^{FGFR1}), renal impairment (classified by estimated glomerular filtration rate [eGFR] by Modification of Diet in Renal Disease formula), and hepatic impairment (classified by the National Cancer Institute Hepatic Dysfunction Working Group) on apparent clearance (CL/F). Also evaluated were the effects of age and baseline body weight on apparent central volume of distribution (V_c/F); baseline body weight on apparent peripheral volume of distribution (V_p/F); and sex, fasting, use of proton pump inhibitors (PPI), and use of histamine two-antagonists (H2B) on the absorption rate constant (K_a).

Covariate selection was performed using a stepwise forward addition process followed by backward elimination. The likelihood ratio test was used to evaluate the significance of including or removing fixed effects into the model. Significance levels for forward addition and backward elimination were 0.05 and 0.005, respectively. Continuous covariates were incorporated into the model using a scaled structure based on either the median value of the covariate in the population or a standard value of the covariate. Categorical covariates were incorporated into the model using proportional structure with the most common level being either the reference level or a level specific to the analysis (e.g., healthy participant vs. patient with disease). A partial block variance–covariance structure for CL/F and V_c/F was evaluated following covariate testing to improve model stability. The final population PK model was evaluated by nonparametric bootstrap analysis and prediction-corrected visual predictive checks.

Exposure-response analyses

Studies and end points

Exposure-response analyses of efficacy and safety in patients with CCA with *FGFR2* fusions/re-arrangements were updated with new data from the now completed FIGHT-202 study.[6]

Serum phosphate and creatinine were measured as part of a comprehensive serum chemistry assessment in FIGHT-101, FIGHT-102, and FIGHT-202. Change from baseline in mean serum phosphate concentration and mean creatinine concentration (mean of cycle 1 day 8 [C1D8] and cycle 1 day 15 [C1D15]) were determined using pooled data from monotherapy patients in the three studies.

For efficacy analyses, objective response rate (ORR) and progression-free survival (PFS) were assessed in patients with CCA who had *FGFR2* fusions/re-arrangements from the FIGHT-202 study.[6] ORR was defined as the percentage of participants in the analysis population who had a confirmed complete response or partial response based on review of scans by an independent centralized radiologic review committee per Response Evaluation Criteria in Solid Tumors (RECIST) version 1.1 results.[16] PFS was defined as the time from first dose to first documented disease progression per RECIST version 1.1 based on independent central review, or death from any cause, whichever occurred first.

Data from the FIGHT-101, FIGHT-102, and FIGHT-202 studies were pooled for safety analyses. Treatment-emergent adverse events (TEAEs) were evaluated in patients who received greater than or equal to one dose of pemigatinib and included the Medical Dictionary for Regulatory Activities (MedDRA) preferred terms

hyperphosphatemia, diarrhea, alopecia, fatigue, dry mouth, stomatitis, constipation, dysgeusia, nausea, decreased appetite, and vomiting. They also included the sponsor-defined clinically notable adverse events (CNAEs) hyperphosphatemia, hypophosphatemia, and retina-related and nail-related toxicities, which are defined as similar preferred terms likely representing a single clinical entity (e.g., hyperphosphatemia and blood phosphorous increased).

Exposure-response evaluation

NONMEM 7.5 was used to simulate a dense steady-state post hoc concentration-time profile for each patient using the updated population PK model. Pemigatinib exposure metrics of maximum observed plasma concentration at steady-state ($C_{max,ss}$), minimum plasma concentration at steady-state ($C_{min,ss}$), and area under the plasma concentration-time curve at steady-state (AUC_{ss}) were derived from the model using noncompartmental methods.

A three-parameter maximum-exposure (E_{max}) nonlinear model was used to evaluate serum phosphate or creatinine concentrations, or percentage change of serum phosphate or creatinine from baseline, as a function of pemigatinib AUC_{ss}. Serum phosphate at baseline was entered into the model as a covariate. The E_{max} model was parameterized in terms of the maximum change in serum phosphate (or creatinine) concentration from baseline (at C1D8 and C1D15 for phosphate) attributed to pemigatinib exposure (E_{max}), and the exposure level of pemigatinib producing 50% of the maximum increase in serum phosphate (or creatinine) concentration from baseline.

A logistic regression model was used to evaluate the relationship between ORR and steady-state pemigatinib plasma exposures and with serum phosphate change from baseline. Kaplan–Meier method was used to evaluate the magnitude of the pemigatinib effects among stratified pemigatinib exposures or serum phosphate concentration change from baseline quartiles. A stratified Cox proportional hazard model with Efron's method of tie handling was used to validate the exposure-PFS relationship.

A logistic regression model was used to evaluate the relationship between pemigatinib plasma exposures at steady-state with the occurrence of TEAEs and CNAEs that were selected within the scope. To evaluate the association between pemigatinib exposure and hyperphosphatemia, a covariate selection process was conducted with the following potential covariates: age, sex, race, body weight and body mass index at baseline, serum chemistries (albumin, alkaline phosphatase, alanine aminotransaminase, aspartate aminotransaminase, total bilirubin, and serum phosphate) at baseline, eGFR for a standardized body surface area of 1.73 m^2, hepatic function impairment classification based on National Cancer Institute Organ Dysfunction Working Group's algorithm, renal function impairment classification based on eGFR, tumor type (CCA vs. other advanced malignancies), *FGFR2* fusion/re-arrangement status (Yes or Otherwise [negative, not tested, or unknown]), and pemigatinib treatment regimen (continuous once-daily [q.d.] dosing vs. intermittent dosing [2 weeks on/1 week off]). E-R analyses were performed in SAS version 9.4 (SAS Institute Inc.).

RESULTS

Population PK dataset

The PK analysis dataset had 4552 concentration records from 467 patients and participants. Mean (SD) age was 54.3 (14.5) years, 46.9% were men, 89.3% received pemigatinib monotherapy, and 16.7% were healthy participants. Tumor types were CCA (34.9%), MLN^{FGFR1} (7.3%), and other cancers (41.1%; Table 1).

Population PK analysis

Concentration-time plots indicated a biphasic decline of concentration over time, supportive of a two-compartment model structure. Normalized concentration profiles showed the lowest concentration for healthy volunteers and the highest for solid tumors, indicating that pemigatinib exposure may be related to tumor types.

A sequential absorption model with a zero-order D1 and first-order K_a provided a stable model with significant fit improvement versus the previous model, which described absorption as a first-order process without a lag time. Objective function values of the base and sequential absorption models were −872.76 and −2262.23, respectively. Based on these findings, the updated base model was determined to be a two-compartment model with sequential zero- and first-order absorption, linear elimination, and an additive residual error on the logarithmic scale. No variance–covariance relationships were identified. All parameters were well estimated with the highest percent relative standard error (%RSE) of 22.2% for the interindividual variability (IIV) on the V_p/F. The highest IIV estimated was 137% for first-order K_a. Following stepwise forward addition and backward elimination, the following covariates were found to have a significant effect on the model PK parameters: sex, use of phosphate binders, and tumor type on CL/F; use of PPI and sex on K_a; use of H2B on D1; and baseline body weight on V_c/F and V_p/F.

TABLE 1 Baseline patient characteristics and covariate summary (population PK analysis).

Covariate	Patients[a] (*n* = 389)	Healthy participants (*n* = 78)	Total (*N* = 467)
Age, years			
Mean (SD)	58.2 (12.1)	34.9 (9.1)	54.3 (14.5)
Median (range)	60.0 (21.0–83.0)	33.5 (19.0–55.0)	56.0 (19.0–83.0)
Baseline body weight, kg			
Mean (SD)	75.2 (20.7)	78.2 (13.3)	75.7 (19.7)
Median (range)	72.6 (39.8–156)	79.7 (50.8–122)	73.9 (39.8–156)
Men, *n* (%)	172 (44.2)	47 (60.3)	219 (46.9)
Tumor type, *n* (%)			
Healthy participant	0	78 (100.0)	78 (16.7)
CCA	163 (41.9)	0	163 (34.9)
MLN	34 (8.7)	0	34 (7.3)
Other	192 (49.4)	0	192 (41.1)
Phosphate binder use,[b] *n* (%)	61 (15.7)	0	61 (13.1)
CYP3A4 inducers, *n* (%)			
None	352 (90.5)	78 (100.0)	430 (92.1)
Weak	36 (9.3)	0	36 (7.7)
Moderate	1 (0.3)	0	1 (0.2)
CYP3A4 inhibitors, *n* (%)			
None	277 (71.2)	78 (100.0)	355 (76.0)
Weak	98 (25.2)	0	98 (21.0)
Moderate	14 (3.6)	0	14 (3.0)
Renal impairment, *n* (%)			
Unimpaired	184 (47.3)	66 (84.6)	250 (53.5)
Mild	157 (40.4)	12 (15.4)	169 (36.2)
Moderate	48 (12.3)	0	48 (10.3)
Hepatic impairment, *n* (%)			
Unimpaired	263 (67.6)	76 (97.4)	339 (72.6)
Mild	114 (29.3)	2 (2.6)	116 (24.8)
Moderate	12 (3.1)	0	12 (2.6)
PPI use, *n* (%)	114 (29.3)	0	114 (24.4)
H2B use, *n* (%)	39 (10.0)	0	39 (8.4)
Pemigatinib monotherapy, *n* (%)	339 (87.1)	78 (100.0)	417 (89.3)

Abbreviations: CCA, cholangiocarcinoma; CYP, cytochrome P450; H2B, histamine 2; MLN, myeloid/lymphoid neoplasms; PK, pharmacokinetics; PPI, proton pump inhibitor.

[a]Patients had CCA, other solid tumors, or MLN.

[b]Binder pertains to phosphate-binding agents.

Final model refinement steps included IIV on V_p/F fixed to 0, removing tumor type on CL/*F* as a covariate (because the 95% CI for both parameters included 0), and introduction of a partial omega block due to the correlation between IIV on CL/*F* and V_c/F. The final PK model successfully minimized, had a successful covariance step, and showed unbiased goodness-of-fit plots (Figure S1). Parameter estimates from the final model are presented in Table 2. Overall, fixed and random-effect parameters were estimated with good precision (%RSE, <19%) except for the coefficient on the effect of H2B use on D1 (%RSE, 38.9%). The final population PK model generally predicted the median and the 5th and 95th percentiles of observed pemigatinib concentrations accurately (Figure 1). Given q.d. dosing regimens for pemigatinib, tight alignments between predicted and observed percentiles from predose up

TABLE 2 Parameter estimates and standard errors from the final population PK model.

	Final parameter estimate			Magnitude of interindividual variability (%CV)			
Parameter	Population Mean	%RSE	95% CI	Final estimate	%RSE	95% CI	Shrinkage, %
CL/*F*, L/h	10.7	2.7	10.1, 11.3	44.8	4.6	40.6, 48.7	4.84
V_c/F, L	118	3.4	110, 125	43.7	8.3	35.9, 50.4	20.6
CL/*F*_V_c/F[a] correlation coefficient, CV	—	—	—	0.659	6.6	—	—
V_p/F, L	95.0	3.0	89.4, 101	Fixed to 0	N/A	N/A	N/A
Q/F, L/h	25.2	7.7	21.4, 29.0	Fixed to 0	N/A	N/A	N/A
K_a, 1/h	3.67	12.2	2.79, 4.55	130	6.0	113, 144	27.7
D1, h	0.810	3.0	0.763, 0.857	60.9	5.2	54.4, 66.8	45.0
RUV, %	—	—	—	32.3	3.0	30.4, 34.1	12.0
Phosphate binder on CL/*F*, %	−15.5	14.6	−19.9, −11.1	—	—	—	—
PPI on K_a, %	−62.0	12.2	−76.8, −47.2	—	—	—	—
Male sex on CL/*F*, %	26.2	18.5	16.7, 35.8	—	—	—	—
Male sex on K_a, %	−58.3	11.1	−71.0, −45.6	—	—	—	—
H2B antagonist on D1, %	−33.4	38.9	−58.9, −8.0	—	—	—	—
Body weight on V_c/F, %	0.842	14.3	0.605, 1.08	—	—	—	—
Body weight to V_p/F, %	1.13	13.0	0.842, 1.42	—	—	—	—

Abbreviations: CL/*F*, apparent clearance; CI, confidence interval; CV, coefficient of variation; D1, duration of zero-order drug release; H2B, histamine 2; K_a, absorption rate constant; N/A, not applicable; PK, pharmacokinetic; PPI, proton pump inhibitor; Q/F, apparent intercompartmental clearance; RSE, relative standard error; RUV, residual unexplained variability; V_c/F, apparent central volume of distribution; V_p/F, apparent peripheral volume of distribution.

[a]CL/*F*_V_c/F covariance was 0.129 with %RSE of 13.6.

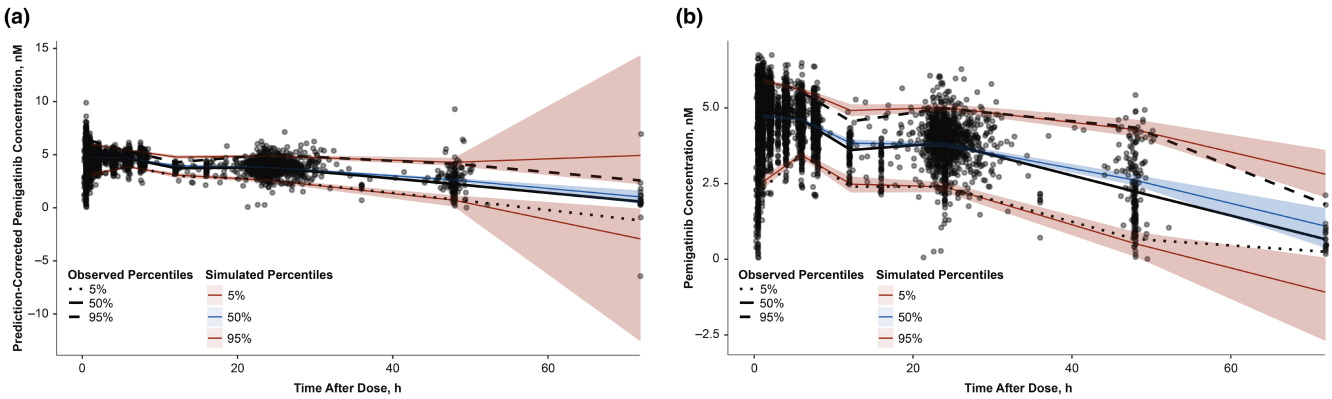

FIGURE 1 (a) Prediction-corrected and (b) Ordinary visual predictive check for the final population PK model. Black dots represent observed data points, the solid black line indicates the observed median, and the black dashed lines show the observed p5 and p95. The blue area represents the 95% PI of the simulated median, and pink areas indicate the 95% PI of the simulated p5 and p95. CI, confidence interval; PI, prediction interval; PK, pharmacokinetics; p5, 5th percentile; p95, 95th percentile.

to ≈50 h suggest that the final population PK model adequately characterized and predicted pemigatinib PKs.

Several covariates impacted pemigatinib PK parameters and exposure (Table 2; Figure S2). Use of phosphate-binding agents resulted in a reduction of 15.5% in CL/*F*, although this was not considered clinically significant. Simulation studies showed that the expected $C_{max,ss}$ of pemigatinib increased by ≈6% in participants who used a phosphate binder compared with nonusers. Men were estimated to have a 26.2% higher CL/*F* and 58.3% lower K_a compared with women. Compared with men, simulated $C_{min,ss}$ and $C_{max,ss}$ were ≈16% and ≈35% higher in women. Use of H2B and PPI resulted in an estimated 33.4% reduction in D1 and 62.0% reduction in K_a, respectively. In simulated exposure studies among observed individuals, concomitant PPI use was predicted to result in ≈20% reduction in $C_{max,ss}$ and ≈9% increase in $C_{min,ss}$. Simulated $C_{max,ss}$ values were 12% lower and 1.1% higher, respectively, in typical PPI or H2B users

versus nonusers. $C_{min,ss}$ values were similar irrespective of concomitant medication use. These results suggest that differences in steady-state exposures due to PPI or H2B use are not clinically significant. Renal impairment, hepatic impairment, and use of weak or moderate CYP3A4 inhibitors or inducers did not significantly impact pemigatinib clearance. Only 12 patients had moderate hepatic impairment in this analysis, which prevented comparisons of CL/*F* in these patients versus other groups. Overall, the impact of demographics, tumor type, creatinine clearance, clinical laboratory values, concomitant medication, renal or hepatic impairment, and *FGFR2* re-arrangement or fusion on pemigatinib exposures was not clinically significant.

Exposure-response analysis of efficacy

The relationship between pemigatinib exposure and change in serum phosphate concentration was evaluated in 300 monotherapy patients. Serum phosphate increases were dependent on pemigatinib exposure and followed a sigmoidal relationship. Serum phosphate concentration at baseline was a significant predictor of the change from baseline in serum phosphate end point. For every 1-mg/dL increase in baseline serum phosphate level, the reduction from baseline was less than or equal to 0.185 mg/dL (Table S2). The pemigatinib exposure that produced 50% of the maximum phosphate concentration was 1665 h·nM, which approximates the mean area under the plasma concentration-time curve from 0–24 h ($AUC_{0\text{-}24h}$) from 8 mg q.d. pemigatinib; therefore, serum phosphate concentration can be used as a surrogate to evaluate the E-R relationships after pemigatinib treatment (Figure 2).

The associations between ORR and PFS and (1) mean change from baseline in serum phosphate concentration and (2) pemigatinib exposure were evaluated in 108 and 103 patients with CCA with *FGFR2* fusions/re-arrangements, respectively. Consistent with the previous analysis, the relationship between ORR and mean change from baseline in serum phosphate concentration followed a bell-shaped curve (Figure 3a).[6] The model predicted ORR of 29.7%, 41.4%, 47.1%, and 46.8% at pemigatinib doses of 6, 9, 13.5, and 20 mg, respectively, suggesting that 13.5 mg is an optimal dose for clinical development. The relationship between ORR and pemigatinib exposure (AUC_{ss}, $C_{max,ss}$, and $C_{min,ss}$) also followed a bell-shaped curve (AUC_{ss} shown in Figure 3b). The model predicted an ORR of 45.2% at a dose of 13.5 mg pemigatinib based on the mean AUC_{ss} of 2850 h·nM at 13.5 mg pemigatinib q.d.

PFS was not associated with mean change from baseline in serum phosphate concentration. The estimates of median PFS were similar for the pemigatinib AUC_{ss} first quartile (6.93 months), second quartile (6.93 months), and fourth quartile (7.03 months) but higher in the third quartile (9.20 months; Figure S3A). However, correlations between pemigatinib exposure (AUC_{ss}, $C_{max,ss}$, or $C_{min,ss}$) and PFS were not significant ($p = 0.68$, 0.44, and 0.46, respectively; Figure S3B).

Exposure-response analysis of safety

Pemigatinib inhibits the membrane transporters OCT2 (50% inhibitory concentration [IC_{50}], 0.075 μM) and MATE1 (IC_{50}, 1.1 μM), suggesting that increased

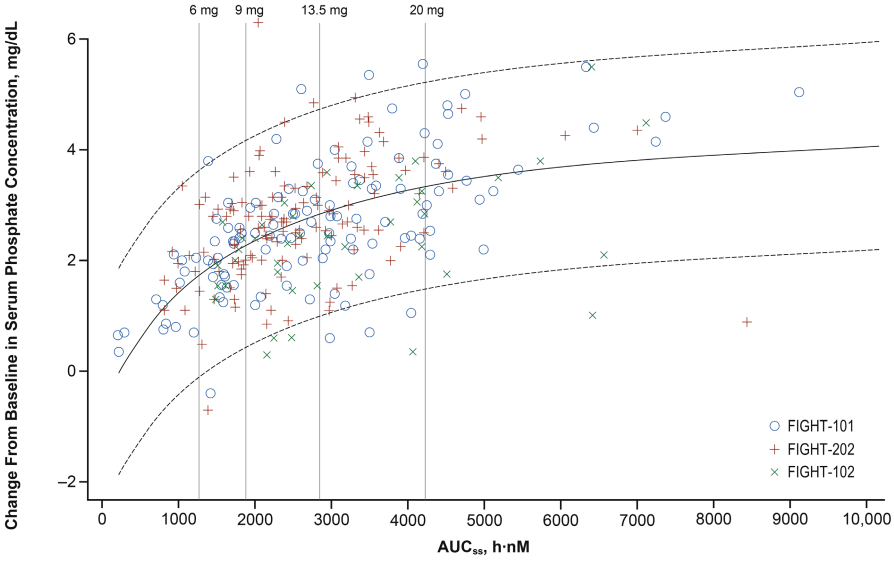

FIGURE 2 Model-predicted versus observed mean serum phosphate concentration change from baseline at C1D8 and C1D15 following once-daily dosing of pemigatinib as monotherapy. The solid black curved line represents the simulated mean, and the dashed black curved lines represent the simulated 5% and 95% percentiles. AUC_{ss}, area under the concentration-time curve at steady-state; C, cycle; D, day.

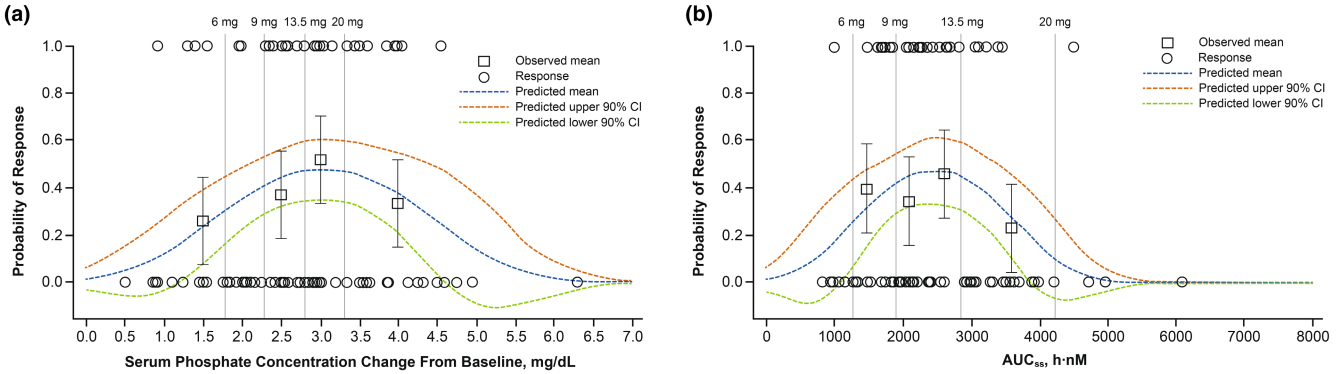

FIGURE 3 Probability of objective response vs (a) mean serum phosphate concentration change from baseline at C1D8 and C1D15 and (b) pemigatinib AUC_{ss} following once-daily dosing of 13.5 mg pemigatinib. Patients received a single daily dose of 13.5 mg pemigatinib. In (a), black squares represent observed first (0.5–2.1 mg/dL), second (2.1–2.7 mg/dL), third (2.7–3.5 mg/dL), and fourth (3.5–6.3 mg/dL) quartiles of serum phosphate concentration change from baseline. In (b), black squares represent first (817–1828 h·nM), second (1828–2351 h·nM), third (2351–3104 h·nM), and fourth (3104–8446 h·nM) quartiles of pemigatinib AUC_{ss}. AUC_{ss}, area under the concentration-time curve at steady-state; C, cycle; D, day.

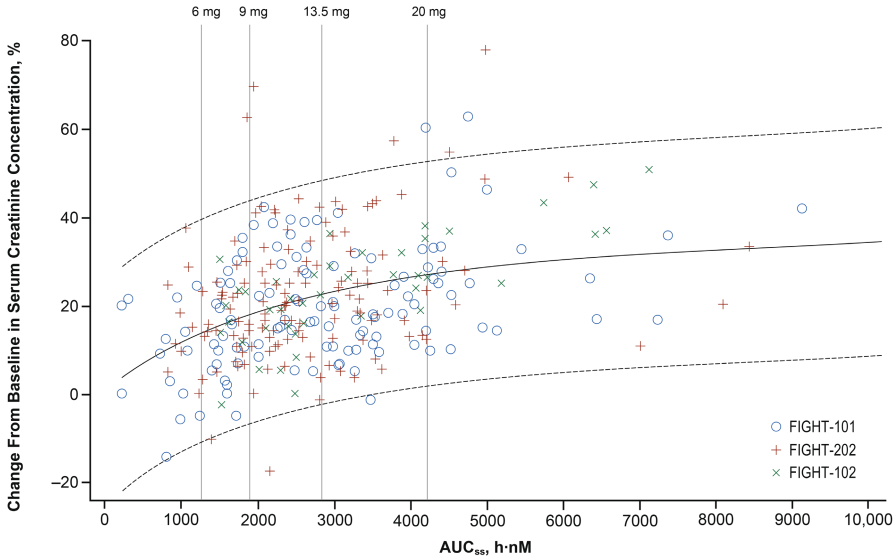

FIGURE 4 Model-predicted versus observed mean serum creatinine concentration percent change following once-daily dosing of pemigatinib as monotherapy. The solid black curved line represents the simulated mean, and the dashed black curved lines represent the simulated 5% and 95% percentiles. AUC_{ss}, area under the concentration-time curve at steady-state.

exposure may increase serum creatinine.[17,18] The relationship between pemigatinib exposure and percentage change from baseline in serum creatinine concentration was evaluated in 300 monotherapy patients. The E_{max} model demonstrated that the increase in serum creatinine observed after treatment with pemigatinib was exposure-dependent and followed a sigmoidal relationship (Table S2). The estimated percentage change from baseline in serum creatinine concentration was 14.2%, 18.3%, 22.7%, and 26.9% at doses of 6, 9, 13.5, and 20 mg, respectively, based on the mean post hoc AUC_{ss} for the dose group of 13.5 mg q.d. and the dose-scaled mean post hoc AUC_{ss} for other dose groups of 6, 9, and 20 mg (Figure 4).

Hyperphosphatemia was evaluated in 305 patients with solid malignancies (CCA with *FGFR2* fusions/re-arrangements, $n = 104$) who received pemigatinib monotherapy. All steady-state exposure metrics ($C_{max,ss}$, $C_{min,ss}$, and AUC_{ss}) were significantly associated with the TEAE and CNAE of hyperphosphatemia; AUC_{ss} had the strongest association. For clinically notable hyperphosphatemia, the parameter estimate for log of AUC_{ss} was 1.40 $(\log \text{ of h·nM})^{-1}$ ($p < 0.0001$), with an odds ratio (OR) for the probability of incidence of hyperphosphatemia estimated to be 1.76 (95% CI, 1.40–2.21) for a 50% increase in AUC_{ss}. Baseline serum phosphate and serum albumin were positively associated with the probability of hyperphosphatemia. The ORs for the probability of incidence of

clinically notable hyperphosphatemia were 2.46 (95% CI, 1.32–4.55) and 4.94 (95% CI, 2.14–11.4) for a 50% increase in serum phosphate and albumin, respectively, at baseline. Conversely, *FGFR2* fusion/re-arrangement status was significantly associated with a lower probability of incidence of clinically notable hyperphosphatemia (OR, 0.498, 95% CI, 0.285–0.870, $p = 0.0144$; Figure 5). Results for the parameter estimates for the TEAE of hyperphosphatemia were similar to those for clinically notable hyperphosphatemia. Neither baseline serum phosphate concentration nor pemigatinib exposure was associated with clinically notable hypophosphatemia.

Nausea, decreased appetite, and stomatitis were significantly associated with pemigatinib exposure, although the associations were generally shallow with the estimated OR less than or equal to 0.052 for every 1-mg increase in pemigatinib dose.

DISCUSSION

A previously developed population PK model was refined using data from seven clinical studies comprising 467 healthy participants and patients with advanced solid tumors including CCA or with MLN^{FGFR1}. The updated population PK model was a two-compartment model with drug dissolution modeled as a zero-order process followed by first-order absorption and first-order elimination. After significant covariate effects were included in the model, the estimated IIV in K_a, D1, CL/F, and V_c/F reflect the typical magnitude expected considering the composition of the PK data used to develop the model. The large IIV in K_a was expected due to high inherent variability in the absorption process and the sparse sampling strategies in FIGHT-102 and FIGHT-202.

As with the original population PK model, covariate analysis identified significant effects between sex and use of phosphate-binding agents on CL/F, sex on K_a, and baseline body weight on V_c/F and V_p/F. The current PK model also identified use of PPI on K_a and use of H2B on D1 as significant covariates. Although these covariates impacted PK parameters, their impact on PK exposures was not clinically significant. The reduction in CL/F due to phosphate binder use, although not readily explained, is not considered clinically significant. The results suggest that phosphate binders can be used to manage hyperphosphatemia with no impact on pemigatinib dosing.

The lower K_a for men versus women is not easily explained. The simulated steady-state peak and trough exposures were higher in women than in men, possibly due to men having higher body weight than women and consequently higher V_c/F. A noncompartmental PK analysis of data from the FIGHT-101 study found that time to C_{max} was statistically different between women and men.

In addition, K_a values for patients on concomitant PPIs were 62% lower compared to patients without PPI use, which is consistent with the previously characterized pH-dependent solubility (poorly soluble at pH > 2) and high permeability of pemigatinib. PPIs decrease gastric acid by inhibiting the H^+/K^+-ATPase responsible for acid secretion in parietal cells.[19] In simulated exposure analyses, concomitant PPI use did not predict clinically significant changes in

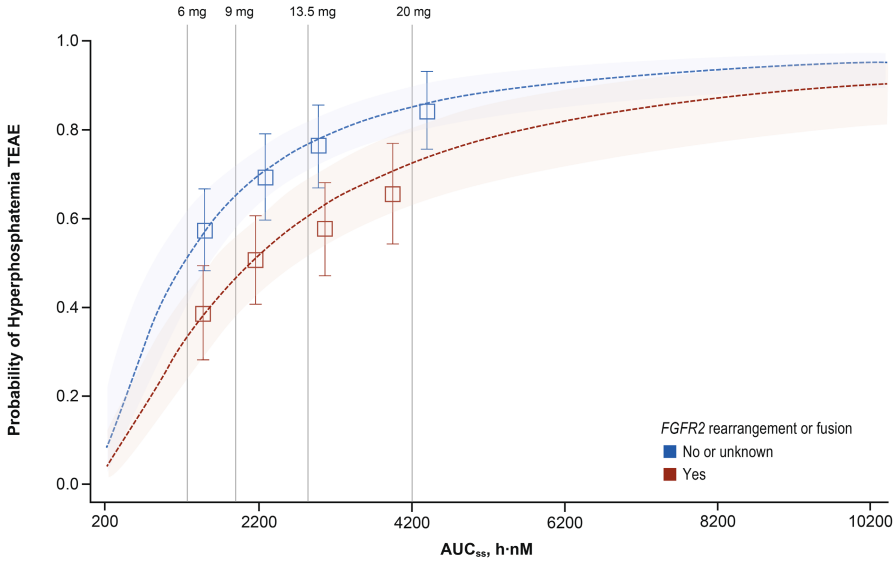

FIGURE 5 Probability of incidence of clinically notable hyperphosphatemia vs pemigatinib AUCss following once-daily dosing of pemigatinib. The squares represent the observed incidence rate at the first, second, third, and fourth quartiles of mean pemigatinib AUC_{ss}. Error bars represent 90% CIs. AUC_{ss}, area under the concentration-time curve at steady-state; CI, confidence interval; FGFR, fibroblast growth factor receptor; TEAE, treatment-emergent adverse event.

$C_{max,ss}$ or $C_{min,ss}$. Additionally, concomitant administration of the PPI esomeprazole had only a modest effect on pemigatinib exposure in the FIGHT-106 study.[12]

H2B also increase stomach pH by inhibiting histamine-mediated gastric acid secretion.[19] In our analysis, concomitant H2B use predicted lower D1. In FIGHT-106, which used serial dense PK sampling, co-administration of the H2B ranitidine resulted in a 2% reduction and 3% increase in C_{max} and AUC, respectively.[12] Sparse PK sampling, limited number of patients who received H2B, and the inclusion of only monotherapy data from FIGHT-106 in this study confound the H2B results. Other factors, such as different potencies and doses of PPI and H2B used by patients in our analysis may have affected the pemigatinib PK. Based on the results of the dedicated drug–drug interaction study FIGHT-106, pemigatinib can be dosed without regard for concomitant H2B use.[12]

Renal and hepatic impairment were not previously shown to be significant predictors of pemigatinib CL/*F*. Previous urine PK analysis in FIGHT-101[5] and FIGHT-105 demonstrated that renal clearance of pemigatinib was 1% to 2% of total clearance,[20] suggesting that mild or moderate renal impairment would minimally affect pemigatinib PKs. In the current study, mild or moderate renal impairment did not significantly impact CL/*F*. Pemigatinib is primarily cleared by the liver;[12] however, post hoc CL/*F* estimates were similar between patients with mildly impaired and unimpaired hepatic function. Overall, pemigatinib dose adjustments are not required in patients with mild or moderate renal or hepatic impairment.

Previous physiologically-based PK modeling showed a greater than 50% increase in pemigatinib AUC when co-administered with moderate or strong CYP3A4 inhibitors, and no drug–drug interaction between pemigatinib and a mild CYP3A4 inhibitor.[12,18] As only 14 patients with concomitant moderate CYP3A4 inhibitor use were included in this population PK analysis, no changes to the recommendation to adjust the dose of pemigatinib with concomitant use of moderate or strong CYP3A4 inhibitors are indicated. No dose adjustments are recommended for co-administration of pemigatinib with weak CYP3A4 inducers. There was insufficient data in the current analysis to provide recommendations for dose adjustment based on concomitant use of CYP3A4 inducers. However, based on the previous drug–drug interaction study of rifampin co-administration,[12,18] concomitant use of strong CYP3A4 inducers with pemigatinib should be avoided.

Consistent with evidence that FGFR inhibition increases serum phosphate concentrations,[9] our analysis indicated that serum phosphate concentration can be used as a surrogate for pemigatinib exposure. Upon regression analysis, both change from baseline in serum phosphate concentration and steady-state pemigatinib exposure were associated with ORR in a bell-shaped relationship. The models suggest that ORR increases before critical values are reached in both serum phosphate concentration change and pemigatinib exposure. Lower ORR observed at higher than median values (>2.7-mg/dL increase from baseline in serum phosphate) may reflect the relatively high incidence rates for dose interruption and dose reduction in this concentration range due to toxicity of FGFR inhibition at high doses. Both models predicted 13.5 mg as the optimal pemigatinib dose, which balances the antitumor effect of FGFR inhibition with the risk of developing TEAEs that require patients to reduce or stop pemigatinib treatment.

Active tubular secretion of creatinine in the kidneys is mediated by multiple membrane transporters, including OCT2, MATE1, and MATE2.[21] In vitro studies have demonstrated that pemigatinib is an inhibitor of OCT2 and MATE1, suggesting that pemigatinib may increase serum creatinine. The exposure-dependent transient and mild creatinine increases observed suggest reversible inhibition of renal excretion transporters by pemigatinib and are consistent with the effect on creatinine through the OCT2/MATE clearance pathway.

The TEAE and CNAE of hyperphosphatemia were both significantly associated with pemigatinib exposure. Higher baseline serum phosphate and albumin concentrations were strong predictors of clinically notable hyperphosphatemia. Intuitively, higher baseline levels of phosphate would translate into a higher probability of elevated serum phosphate levels on treatment. High albumin levels typically result from dehydration. Under such conditions, the volume of circulating blood is expected to be lower and the phosphate level in serum is anticipated to be elevated. Interestingly, we found that patients with CCA and *FGFR2* fusions/re-arrangements experienced significantly lower incidences of the TEAE and CNAE of hyperphosphatemia than patients with CCA without *FGFR2* alterations or patients with other malignancies. The physiologic interpretation of such effects is not clear.

The lack of statistically significant correlation between pemigatinib exposure and other evaluated TEAEs could be due to the narrow dose range explored and the relatively low frequency of TEAEs, such as constipation and vomiting.

CONCLUSIONS

Pemigatinib PK was described a two-compartment model with sequential zero- and first-order absorption and linear elimination. Based on this analysis, no dose adjustments for pemigatinib are recommended for concomitant of use of PPI, H2B, weak CYP3A4 inhibitors or inducers, or patients with mild or moderate renal or hepatic impairment. E-R analyses demonstrated that higher pemigatinib

exposure at steady-state and baseline serum phosphate concentrations were associated with both increased hyperphosphatemia and ORR. Overall, we showed that pemigatinib 13.5 mg q.d. in 21-day cycles (2 weeks on/1 week off) offers a favorable benefit–risk profile in patients with advanced/metastatic or surgically unresectable CCA and is the optimal dose for clinical development.

AUTHOR CONTRIBUTIONS

All authors wrote the manuscript. X.G., T.J., X.L., and X.C. designed the research. All authors performed the research and analyzed the data.

ACKNOWLEDGMENTS

Writing assistance was provided by Erin McClure, PhD, an employee of ICON (Blue Bell, PA, USA).

FUNDING INFORMATION

This study was funded by Incyte Corporation (Wilmington, DE, USA).

CONFLICT OF INTEREST STATEMENT

X.G., X.L., and X.C. are employees and shareholders of Incyte. A.A., A.N., and M.L. are employees of Certara. T.J. was an employee of Incyte at the time of the study and a current employee of Allorion Therapeutics.

REFERENCES

1. Xie Y, Su N, Yang J, et al. FGF/FGFR signaling in health and disease. *Signal Transduct Target Ther*. 2020;5:181.
2. Babina IS, Turner NC. Advances and challenges in targeting FGFR signalling in cancer. *Nat Rev Cancer*. 2017;17:318-332.
3. Murugesan K, Necchi A, Burn TC, et al. Pan-tumor landscape of fibroblast growth factor receptor 1-4 genomic alterations. *ESMO Open*. 2022;7:100641.
4. Reiter A, Gotlib J. Myeloid neoplasms with eosinophilia. *Blood*. 2017;129:704-714.
5. Subbiah V, Iannotti NO, Gutierrez M, et al. FIGHT-101, a first-in-human study of potent and selective FGFR 1-3 inhibitor pemigatinib in pan-cancer patients with FGF/FGFR alterations and advanced malignancies. *Ann Oncol*. 2022;33:522-533.
6. Abou-Alfa GK, Sahai V, Hollebecque A, et al. Pemigatinib for previously treated, locally advanced or metastatic cholangiocarcinoma: a multicentre, open-label, phase 2 study. *Lancet Oncol*. 2020;21:671-684.
7. Gotlib J, Kiladjian JJ, Vannucchi A, et al. A phase 2 study of pemigatinib (FIGHT-203; INCB054828) in patients with myeloid/lymphoid neoplasms (MLNs) with fibroblast growth factor receptor 1 (FGFR1) rearrangement (MLN FGFR1). *Blood*. 2021;138:385.
8. Verstovsek S, Gotlib J, Vannucchi AM, et al. FIGHT-203, an ongoing phase 2 study of pemigatinib in patients with myeloid/lymphoid neoplasms (MLNs) with fibroblast growth factor receptor 1 (FGFR1) rearrangement (MLNFGFR1): a focus on centrally reviewed clinical and cytogenetic responses in previously treated patients. *Blood*. 2022;140:3980-3982.
9. Mahipal A, Tella SH, Kommalapati A, Yu J, Kim R. Prevention and treatment of FGFR inhibitor-associated toxicities. *Crit Rev Oncol Hematol*. 2020;155:103091.
10. PEMAZYRE® (pemigatinib). Full prescribing information, Incyte Corporation, Wilmington, DE, USA. 2022.
11. Ji T, Lihou C, Asatiani E, et al. Pharmacokinetics and pharmacodynamics of pemigatinib, a potent and selective inhibitor of FGFR 1, 2, and 3, in patients with advanced malignancies. AACR-NCI-EORTC symposium on molecular targets and cancer therapeutics; 2019 October 26–30; Boston, MA.
12. Ji T, Rockich K, Epstein N, et al. Evaluation of drug-drug interactions of pemigatinib in healthy participants. *Eur J Clin Pharmacol*. 2021;77:1887-1897.
13. Ji T, Rockich K, Epstein N, et al. Evaluation of the pharmacokinetics of pemigatinib in patients with impaired hepatic or renal function. *Br J Clin Pharmacol*. 2022;88:237-247.
14. Ji T, Chen X, Liu X, Yeleswaram S. Population pharmacokinetics analysis of pemigatinib in patients with advanced malignancies. *Clin Pharmacol Drug Dev*. 2022;11:454-466.
15. R Core Team. *R: A Language and Environment for Statistical Computing*. R Foundation for Statistical Computing; 2023.
16. Eisenhauer EA, Therasse P, Bogaerts J, et al. New response evaluation criteria in solid tumours: revised RECIST guideline (version 1.1). *Eur J Cancer*. 2009;45:228-247.
17. Chu X, Bleasby K, Chan GH, Nunes I, Evers R. The complexities of interpreting reversible elevated serum creatinine levels in drug development: does a correlation with inhibition of renal transporters exist? *Drug Metab Dispos*. 2016;44:1498-1509.
18. Ji T, Chen X, Yeleswaram S. Evaluation of drug-drug interaction potential for pemigatinib using physiologically based pharmacokinetic modeling. *CPT Pharmacometrics Syst Pharmacol*. 2022;11:894-905.
19. Maret-Ouda J, Markar SR, Lagergren J. Gastroesophageal reflux disease: a review. *JAMA*. 2020;324:2536-2547.
20. European Medicines Agency. Assessment report: Pemazyre. February 25, 2021; 1–136. Accessed May 3, 2023. https://www.ema.europa.eu/en/documents/assessment-report/pemazyre-epar-public-assessment-report_en.pdf
21. Chappell JC, Turner PK, Pak YA, et al. Abemaciclib inhibits renal tubular secretion without changing glomerular filtration rate. *Clin Pharmacol Ther*. 2019;105:1187-1195.

SUPPORTING INFORMATION

Additional supporting information can be found online in the Supporting Information section at the end of this article.

How to cite this article: Gong X, Akil A, Ndi A, et al. Population pharmacokinetic and exposure-response analyses of pemigatinib in patients with advanced solid tumors including cholangiocarcinoma. *CPT Pharmacometrics Syst Pharmacol*. 2023;12:1784-1794. doi:10.1002/psp4.13064